Geodetic constraints on active tectonics of the Western Mediterranean: Implications for the kinematics and dynamics of the Nubia-Eurasia plate boundary zone

Philippe Vernant, Abdelali Fadil, Taoufik Mourabit, Driss Ouazar, Achraf Koulali, Jose Martin Davila, Jorge Garate, Simon Mcclusky, Robert Reilinger

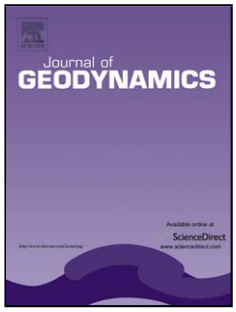

Title: Geodetic constraints on active tectonics of the Western Mediterranean: Implications for the kinematics and dynamics of the Nubia-Eurasia plate boundary zone

Authors: Philippe Vernant, Abdelali Fadil, Taoufik Mourabit, Driss Ouazar, Achraf Koulali, Jose Martin Davila, Jorge Garate, Simon McClusky, Robert Reilinger

PII: S0264-3707(09)00118-5
DOI: doi:10.1016/j.jog.2009.10.007
Reference: GEOD 945

To appear in: *Journal of Geodynamics*

Received date: 30-1-2009
Revised date: 25-6-2009
Accepted date: 6-10-2009

Please cite this article as: Vernant, P., Fadil, A., Mourabit, T., Ouazar, D., Koulali, A., Davila, J.M., Garate, J., McClusky, S., Reilinger, R., Geodetic constraints on active tectonics of the Western Mediterranean: Implications for the kinematics and dynamics of the Nubia-Eurasia plate boundary zone, *Journal of Geodynamics* (2008), doi:10.1016/j.jog.2009.10.007

Geodetic constraints on active tectonics of the Western Mediterranean: Implications for the kinematics and dynamics of the Nubia-Eurasia plate boundary zone

Philippe Vernant, Geosciences Montpellier, CNRS-University of Montpellier, Montpellier, FRANCE, pvernant@um2.fr

Abdelali Fadil, Geodesy Observatory, University of French Polynesia, TAHITI. abdelali.fadil@upf.pf

Taoufik Mourabit, Universite Abdelmalek Essaadi, Tangier, MOROCCO, tmourabit@menara.ma

Driss Ouazar and Achraf Koulali, Ecole Mohammadia des Ingenieurs, Rabat, MOROCCO, ouazar@emi.ac.ma

Jose Martin Davila and Jorge Garate, Real Observatorio de la Armada (Royal Naval Observatory) Cecilio Pujazon s/n, 11100 San Fernando (Cadiz), SPAIN, mdavila@roa.es

Simon McClusky and Robert Reilinger, DEAPS, MIT, Cambridge, MA, USA, reilinge@erl.mit.edu

Abstract

We present GPS observations in Morocco and adjacent areas of Spain from 15 continuous (CGPS) and 31 survey-mode (SGPS) sites extending from the stable part of the Nubian plate to central Spain. We determine a robust velocity field for the W Mediterranean that we use to constrain models for the Iberia-Nubia plate boundary. South of the High Atlas mountain system, GPS motions are consistent with Nubia plate motions from prior geodetic studies. We constrain shortening in the Atlas system to <

1.5 mm/yr, 95% confidence level. North of the Atlas Mountains, the GPS velocities indicate Nubia motion with respect to Eurasia, but also a component of motion normal to the direction of Nubia-Eurasia motion, consisting of southward translation of the Rif Mountains in N Morocco at rates exceeding 5 mm/yr. This southward motion appears to be directly related to Miocene opening of the Alboran Sea. The Betic mountain system north of the Alboran Sea is characterized by WNW motion with respect to Eurasia at ~ 1 – 2 mm/yr, paralleling Nubia-Eurasia relative motion. In addition, sites located in the Betics north of the southerly moving Rif Mountains also indicate a component of southerly motion with respect to Eurasia. We interpret this as indicating that deformation associated with Nubia-Eurasia plate motion extends into the southern Betics, but also that the Betic system may be affected by the same processes that are causing southward motion of the Rif Mountains south of the Alboran Sea. Kinematic modeling indicates that plate boundary geometries that include a boundary through the straits of Gibraltar are most compatible with the component of motion in the direction of relative plate motion, but that two additional blocks (Alboran-Rif block, Betic Mountain block), independent of both Nubia and Eurasia are needed to account for the motions of the Rif and Betic mountains normal to the direction of relative plate motion. We speculate that the southward motions of the Alboran-Rif and Betic blocks may be related to mantle flow, possibly induced by southward rollback of the subducted Nubian plate beneath the Alboran Sea and Rif Mountains.

Introduction

The tectonic evolution of the western Mediterranean has been dominated by the long history of Nubia-Eurasia plate convergence associated with subduction of the Neotethys

oceanic lithosphere (e.g., Dercourt et al., 1986). The current-day tectonic structure of the zone of plate interaction is complex, involving back-thrust mountain ranges on the north (Betics) and south (Rif) sides of the collision zone and an intervening, deep basin (Alboran) reflecting active extension and subsidence (Figure 1). Such juxtaposition of compression and extension is observed along some subduction zones and appears to be associated with retreat (or rollback) of the subducting slab (e.g., Le Pichon and Angelier, 1979, Royden, 1993). However, in the W Mediterranean the evidence for active subduction is equivocal (e.g., Seber et al., 1996, Gutscher et al., 2002, Faccenna et al., 2004).

Geodetic observations have revealed a highly unexpected pattern of deformation within the W Mediterranean zone of plate interaction, indicating southward motion of the Rif Mountains in N Morocco relative to the Nubian plate interior (Fadil et al., 2006). These well-defined, anomalous motions appear to be incompatible with crustal interactions (i.e., extrusion tectonics) and, we suggest, more likely reflect active, sub-crustal processes, possibly associated with subduction and/or mantle delamination within the zone of convergence between Nubia and Iberia (Seber et al., 1996, Gutscher et al., 2002, Fadil et al., 2006). In this paper, we incorporate new observations to update the GPS velocities in Morocco, and we combine these with GPS measurements from southern Spain, and Spanish enclaves in N Africa, to develop an internally consistent velocity field for the W Mediterranean region. We use this improved velocity field to constrain block models of the Nubia-Eurasia plate boundary deformation zone and we discuss the implications of these observations for the dynamics of Nubia-Eurasia plate interactions.

Tectonic setting and active deformation

In the western Mediterranean, the Alboran domain is caught between North Africa and Iberia at the westernmost limit of the Alpine mountain belt (Figure 1). During the Cenozoic, the Alboran domain, along with the Atlas Mountains, grew thicker in this convergent setting (Chalouan and Michard, 2004; Platt and Vissers, 1989). Later during the Miocene, the Alboran domain stretched and subsided below sea level, accumulating more than 7 km of sediment (Watts et al., 1993).

Present-day tectonic processes occur within the context of ongoing, ~NW-SE oblique convergence between Africa and Iberia around the Strait of Gibraltar (4.3 ± 0.5 mm/yr at an azimuth of 116 ± 6° from GPS, Figure 2a (McClusky et al., 2003)). However, the location, or existence, of a discrete Africa-Eurasia plate boundary is equivocal (Figure 1). Geomorphologic studies of active faulting demonstrate recent tectonic activity in the Rif (Morel and Meghraoui, 1996) and the Atlas Mountains (Gomez et al., 1996; Meghraoui et al., 1998; Gomez et al., 2000), and suggest that most of the present-day convergence is accommodated in the Rif-Betic-Alboran region.

Ideas to explain the striking N-S topographical symmetry of the Alboran Sea and surrounding mountain belts, as well as the apparently synchronous subsidence of the Alboran Sea and uplift of the Betic and Rif mountains during the Neogene and Quaternary are still widely debated. Current tectonic models for the Alboran domain include four broad categories of hypotheses: (1) backarc extension driven by the

westward rollback of an eastward subducting slab of oceanic lithosphere (Royden, 1993; Lonergan and White, 1997; Gutscher et al., 2002); (2) break-off of a subducting lithospheric slab (Blanco and Spakman, 1993); (3) crustal extrusion due to forces transmitted across the Eurasia-Africa plate boundary (Rebai et al., 1992; Morel and Meghraoui, 1996); and (4) delamination and convective removal of the lithospheric mantle root beneath the collisional orogen (Platt and Vissers, 1989; Seber et al., 1996; Calvert et al., 2000a; Calvert et al., 2000b). Testing these hypotheses with the present-day deformation field is a principal objective of this study.

GPS Velocities and Data Processing

The GPS network used in this study includes 31 GPS survey points (SGPS) observed for different time intervals between 1999 and 2007, and 15 continuous GPS stations (CGPS, Fig. 2a). We analyze the GPS data using the GAMIT/GLOBK software (Herring, 1999; King and Bock, 1999) in a two-step approach (McClusky et al., 2000). The GPS solution is realized in the ITRF2005 global reference frame, and rotated into a Eurasia and Africa reference frame using 23 and 12 stations respectively. The mean values of the residuals for the eastern and the northern components of the 23 Eurasian sites and 12 African sites are -0.16 mm/yr, 0.15 mm/yr, -0.29 mm/yr and 0 mm/yr respectively, the standard deviation being 0.61 mm/yr, 0.71 mm/yr, 0.42 mm/yr and 0.45 mm/yr. Therefore no significant residuals remain in the reference frame computation, and as shown in Figure

3, most of the residuals are lower than 1mm/yr. Site velocities in both the Eurasia and Africa reference frames are given in Table 1.

Figure 2a shows GPS velocities in a Nubian-fixed reference frame, and Figure 2b, the same solution relative to Eurasia. One-sigma uncertainties for survey sites are mostly < 0.7 mm/yr, and < 0.4 mm/yr for long-operating CGPS stations. GPS velocities at sites located south of the Rif Mountains and north of the High Atlas (SALA, KBGA, HEBR, DEBD, BMTR) are consistent with the motion of Nubia at the 1-sigma confidence interval (Figure 2a; Table 1), implying deformation rates of less than 0.7 mm/yr within the High Atlas Mountains. Uncertainties on these survey sites are too large to detect active shortening. However, the two CGPS sites south of the Rif Mountains and north of the Atlas system (RABT, IFRN) that have more tightly constrained velocities both show significant SSE velocities with respect to Nubia (1.0 ± 0.2 and 1.7 ± 0.3, respectively) that may be due to shortening across the Atlas Mountain system, with a substantial component of shortening in the Middle Atlas. These estimates are within the range of geological rates that constrain shortening to about 1 to 2 mm/yr across the entire Atlas mountain system (Meghraoui et al., 1998; Gomez et al., 2000).

The anomalous motions of the central Rif Mountains in northern Morocco are apparent in the Nubian-fixed velocity map shown in Figure 2a. The central Rif Mountains are moving SSW as defined by 9 survey sites and the continuous station in Tetouan (TETN). Southwest motion of the Rif is largest in the northern and central Rif (5.4 ± 1.5 mm/yr) where topography is highest and decreases to the south, terminating near the northern

boundary of the Atlas system. The western boundary of the southward moving Rif zone appears to be located near station TETN, and the eastern boundary near the Al Hoceima seismic zone.

Motions in southern Spain north of the Alboran Sea are best illustrated by the Eurasia-fixed velocity map shown in Figure 2b. Sites located near the Betic Mountains (ALME, GRAN, MALA, ALGE, SFEB) show well-defined westward motions with respect to Eurasia (~2 mm/yr). Sites COBA and LAGO further north show similar, although slower westward motions (~ 1 mm/yr). Motion of the Betics with respect to Eurasia has a similar orientation to Nubia-Eurasia motion, but with reduced rates, and those sites in the Betics located north of the southward moving central Rif zone (ALME, GRAN, MALA) also show a southerly component of motion relative to Eurasia. These motions imply transtension in the Betics that is consistent with WSW-ENE extension pointed out by Martínez-Martínez et al. (2006) on the base of earthquake focal mechanisms and active faults.

Kinematics of the Nubia-Iberia Interplate Deformation Zone

To illustrate better deformation in the plate boundary zone and the relation to hypothesized plate boundaries, in Figure 4 we plot the components of the GPS velocities normal and parallel to two profiles striking N20°E, roughly perpendicular to the direction of Eurasia-Africa relative motion (~N110°E) (see profile locations on Figure 2a). For the western profile, the velocity component in the direction of Eurasia-Africa motion (i.e., normal to the strike of the profile) clearly shows the relative plate motion (Figure 4a), and

no significant motion normal to the direction of relative plate motion (Figure 4b). We use an elastic block model (McCaffrey, 2002), to investigate the consistency of the observed pattern of motion with the three hypothesized plate boundaries illustrated in Figure 1. The width of the deformation zone across block boundaries depends on the assumed fault-locking depth. We use a locking depth of 15 km for all faults, in agreement with the maximum depth of the seismicity (Calvert et al., 1997; Stich et al., 2003). Model results for the three plate boundary geometries are shown in Figures 4a, 4b, 4d, and 4e. For the westernmost profile (Profile 1) the GPS results are inconsistent with the plate boundary located south of the Rif (Bird, 2003) or north of Gibraltar in the Betic Cordillera (Gutscher, 2004). The best fit is for models where the boundary passes through the Gibraltar Strait (Klitgord and Schouten, 1986). The models predict no significant motion normal to the direction of relative plate motion (N20°E), consistent with the GPS observations, indicating that the westernmost segment of the plate boundary is consistent with simple, elastic plate interactions.

The second, more eastern profile crosses the central Rif, Alboran Sea and Betic Mountains (see location on Figure 2a). As for the western profile, Eurasia/Africa relative motion is apparent (Figure 4d), but the component of velocity normal to the direction of relative plate motion shows anomalous deformation in the Alboran/Rif, and to a lesser extent in the Betics (Figure 4e). None of the proposed plate boundary geometries can account for this motion. Expanding on the models of Fadil et al. (2006), we investigate kinematic models including a central Alboran-Rif block and a Betic block (Figure 5). Most of the block boundaries are consistent with mapped fault zones, or seismic

lineaments. The western and southern boundaries of the Alboran-Rif block are well constrained by the GPS velocities. However, no regional right lateral strike slip faults are reported where we locate the western Rif block boundary. We assign a 15 km locking depth to all block boundaries. Although block models are very useful to identify large quasi-rigid blocks or plates, they have inherent limitations for smaller blocks. Indeed, the width of the interseismic transient elastic strain on one side of a fault in the block model is approximately 3 locking depths (Savage and Burford, 1973). Therefore if the width of a block is less than 6 locking depths, the entire block will deform elastically during the interseismic interval of the seismic cycle making it difficult to identify coherently moving areas (i.e., blocks). Furthermore, it is impossible to unambiguously separate transient elastic strain from permanent geologic deformation for small blocks. This is the case of all the blocks defined in this study. Therefore one should be careful with the fault slip rates given in Figure 5, they are upper bounds since they assume all observed strain is elastic, and depend on how the deformation is accommodated within the regions evidenced by our kinematic analysis.

The southern Alboran-Rif block boundary corresponds to mapped Quaternary thrust faults along the southern edge of the Rif (Moratti et al., 2003). The northern and eastern boundaries of the Rif block are poorly constrained by the GPS results. We have chosen to locate the eastern boundary along the NS trend of the 1994 and 2004 Al Hoceima earthquakes, and the seismically active Alboran Ridge, consistent with most other interpretations (Figure 1). We also include a separate block representing the Betic mountain system. The northern boundary of the Betic block corresponds to the Nubia-

Iberia plate boundary of Gutscher (2004), and the southern boundary to mapped normal faults on the north side of the Alboran Basin. Overall, the block boundaries we propose in Figure 5 are a combination of previously proposed boundaries, finding support from, and capturing aspects of each of these prior interpretations. The predicted interseismic motion along the two profiles for this model is in good agreement with the observed GPS velocities (Figure 4a, b, d, e).

Geodynamic Implications

Present-day motions indicated by GPS in northern Morocco and southern Iberia appear consistent, to first order, with geological indicators of active neotectonic deformation, indicating crustal shortening in the central Rif juxtaposed with extension of the Alboran Sea. Left lateral strike slip rates on NNE striking faults along the east side of the central Rif block in N Morocco derived from our model (~5-6 mm/yr, Figure 5) are roughly consistent with rates reported from studies of active faults in the Rif (Morel and Meghraoui, 1996), as well as with the sense of motion indicated by the 1994 and 2004 Al-Hoceima earthquakes (Calvert et al., 1997; Stich et al., 2003; Tahayt et al., 2008). Furthermore, the N-S width of the deep Alboran Basin is roughly 120 km. Assuming that the GPS extension rate across the basin (roughly 4 mm/yr between stable Nubia and Eurasia, see Figure 4d) has been constant in time, the basin would be formed in about 30 Ma, in good agreement with geological estimates for the beginning of extension at 27 Ma (Platt and Whitehouse, 1999). The southward motion of the Betic block decreases the extension rate confined to the Alboran Sea (from ~4 to ~3 mm/yr, Figure 4e), possibly implying that extension has spread North into the Betics sometime after initial extension

of the Alboran Basin. Martínez-Martínez et al. (2006) point out that the mode of present-day extension in the Betic system must have remained substantially the same over the last ~15 Myr, supporting our contention that the GPS motions reflect those processes responsible for the geologic evolution of the W Mediterranean region.

The general agreement between GPS and geologic indicators of neotectonic deformation suggests that the GPS results depict those geodynamic processes responsible for the geologic evolution of the Betic-Alboran Sea-Rif Mountain system, providing quantitative constraints on models for the evolution of this segment of the Africa-Eurasia plate boundary. The occurrence of extension on fault segments within the zone of Nubia-Iberia plate convergence (i.e., northern Betics, some of the western and eastern boundaries of the Rif block, see Figure 5) appears inconsistent with extrusion models that involve compressive forces transmitted across plate boundaries. Southward motion of the Betic Mountains also appears to be inconsistent with extrusion models since the zone of maximum compresion within the collision zone would be expected to lie south of the Betic system. West-directed roll back of an east dipping subducted slab beneath Gibraltar also appears inconsistent with the SE motion of GPS sites in northwestern Morocco since this model predicts westward motion of the Gibraltar region relative to Africa (Gutscher, 2004).

An alternate geodynamic model for the western Mediterranean proposes that the subcontinental part of the lithosphere under the Alboran domain has been removed by active delamination (e.g., Seber et al., 1996, Calvert et al., 2000). As pointed out by Platt

et al. (2003), simple delamination would produce a radially symmetric pattern of surface deformation (i.e., northward transport of the Betic Mountains). The GPS data indicate that the Betics are, at least at the present time, moving with a southward component of motion relative to Africa (Figure 2b), inconsistent with radially symmetric deformation predicted by active, vertical delamination models.

The observed, southward directed motion of the central Rif, roughly normal to the direction of Africa-Eurasia relative plate motion, and to some extent of the Betic system, supports the hypothesis that subcrustal process are controlling the opening of the Alboran Sea and adjacent shortening in the Rif (Fadil et al., 2006). Based principally on the GPS results, the asymmetric deformation around the Alboran Sea appears to be more indicative of a component of southward-directed slab roll back and associated N-S back arc opening than with simple symmetric delamination confined to the Alboran Sea region. The direction of roll back corresponds to the direction of motion of the inferred Alboran-Rif block (SSW relative to Nubia). Because the Rif-Alboran-Betic region is continental in character (Platt and Vissers, 1989), the present-day slab is probably the mantle part of the continental lithosphere, which has become detached from the crust and is rolling back to the south, possibly due to the pull of the old slab (Faccenna et al., 2004). These considerations support the hypothesis that neotectonic deformation in the western Mediterranean, including juxtaposed extension of the Alboran Sea and uplift of the surrounding mountain ranges, results from dynamic processes in the upper mantle associated with continued convergence of the Nubian and Eurasian plates.

Conclusions

We present the GPS velocity field traversing the Nubia-Eurasia plate boundary in the westernmost Mediterranean and use it to estimate active deformation. We constrain crustal shortening in the High Atlas to ≤ 1 mm/yr, and across the entire Atlas system to ≤ 1.5 mm/yr (95%), and show that the principal deformation associated with Nubia-Eurasia interaction occurs in the Betic-Rif-Alboran domain. With 14 new sites (AION, ALGE, BOYA, CACE, MELI, GRSF, GRAN, MALA, TANT, CRDB, COBA, KTMA, CHEF, CSTL) compared to the earlier velocity field reported by Fadil et al. (2006), we extend GPS coverage to the southern Iberia region, and show that significant displacements occur in the Betic mountain system. We further demonstrate that, while simple elastic plate interactions can account for observed Nubia-Eurasia relative plate motion in the direction of relative plate motion, the observed component of motion normal to this direction requires more complex plate interactions. We argue on the basis of the observed GPS velocities and regional tectonics that neither extrusion tectonics nor simple vertical delamination can easily account for this deformation. We suggest that the kinematics of the region are most simply associate with slab roll-back toward the SSW and back arc opening in the Alboran Basin, superimposed on Eurasia-Nubia differential motion. As the region is now an intra-continental domain, the present-day slab is probably part of the Moroccan lithospheric mantle that has been pulled down and is now delaminating, the zone of delamination being somewhere along the Moroccan Mediterranean shore. The slab must be narrow since the lateral extent of the southward motion is only 150-200 km, making it a challenge to image with seismological methods.

These results emphasize the importance of mantle dynamics in driving lithospheric deformation.

Acknowledgements

We thank UNAVCO for providing equipment and technical support for the surveys in Morocco, and for assistance with establishing and maintaining the continuous GPS station in Rabat. We are grateful to Rob McCaffrey for providing his DEFNODE code, and for assistance with implementation and to C. Facenna and an anonymous reviewer for their helpful reviews. This research was supported in part by NSF Grant EAR-0408728 to MIT, ACOGE_RISTE grant CGL2006-10311-C03-02 and TOPOIBERIA, grantCSD2006-00041 to ROA.

References

Bird, P., 2003, An updated digital model of plate boundaries: *Geochem. Geophys. Geosyst., v. 4*, p. 10.1029/2001GC000252.

Blanco, M.J., and Spakman, W., 1993, The P-wave velocity structure of the mantle below the Iberian Peninsula: Evidence for subducted lithosphere below southern Spain: *Tectonophysics, v. 221*, p. 13-34.

Calvert, A., Gomez, F., Seber, D., Barazangi, M., Jabour, N., Ibenbrahim, A., and Demnati, A., 1997, An integrated geophysical investigation of recent seismicity in the Al-Hoceima region of North Morocco: *Bull. Seismol. Soc. Am., v. 87*, p. 637-651.

Calvert, A., Sandvol, E., Seber, D., Barazangi, M., Roecker, S., Mourabit, T., Vidal, F., Alguacil, G., and Jabour, N., 2000a, Geodynamic evolution of the lithosphere and upper mantle beneath the Alboran region of the western Mediterranean; constraints from travel time tomography: *J. Geophys. Res., v. 105*, p. 10871-10898.

Calvert, A., Sandvol, E., Seber, D., Barazangi, M., Vidal, F., Alguacil, G., and Jabour, N., 2000b, Propagation of regional seismic phases (Lg and Sn) and Pn velocity structure along the Africa-Iberia plate boundary zone; tectonic implications: *Geophys. J. Int., v. 142*, p. 384-408.

Chalouan, A., and Michard, A., 2004, The Alpine Rif Belt (Morocco); a case of mountain building in a subduction-subduction-transform fault triple junction: *Pure Appl. Geophys., v. 161*, p. 489-519.

Dercourt, J., et al., 1986, Geological evolution of the Tethys belt from the Atlantic to the Pamirs since the Lias, *Tectonophysics, 123,* 241-315.

Faccenna, C., Piromallo, C., Crespo-Blanc, A., Jolivet, L., and Rossetti, F., 2004, Lateral slab deformation and the origin of the western Mediterranean arcs: *Tectonics, v. 23*, p. 21,doi: 10.1029/2002TC001488.

Fadil, A., P. Vernant, S. McClusky, R. Reilinger, and 5 others, 2006, Active tectonics of the western Mediterranean: GPS evidence for roll back of a delaminated subcontinental slab beneath the Rif Mountains, Morocco, *Geology, 34*, 529-532, doi:10.1130/G22291.1.

Gomez, F., Barazangi, M., and Bensaid, M., 1996, Active tectonism in the intracontinental middle Atlas Mountains of Morocco; synchronous crustal

shortening extension: *Journal of the Geological Society of London, v. 153*, p. 389-402.

Gomez, F., Beauchamp, W., and Barazangi, M., 2000, Role of the Atlas Mountains (Northwest Africa) within the African-Eurasian plate-boundary zone: *Geology, v. 28*, p. 775-778.

Gutscher, M.-A., 2004, What Caused the Great Lisbon Earthquake?: *Science, v. 305*, p. 1247-1248.

Gutscher, M.A., Malod, J., Rehault, J.P., Contrucci, I., Klingelhoefer, F., Mendes-Victor, L., and Spakman, W., 2002, Evidence for active subduction beneath Gibraltar: *Geology, v. 30*, p. 1071-1074.

Herring, T.A., 1999, GLOBK: Global Kalman filter VLBI and GPS analysis program, version 4.1: Cambridge, Mass. Inst. of Technol.

King, R.W., and Bock, Y., 1999, Documentation for the GAMIT analysis software, release 9.7: Cambridge, Mass. Inst. of Technol.

Klitgord, K.D., and Schouten, H., 1986, Plate kinematics of the central Atlantic, *in* Vogt, P.R., and Tucholke, B.E., eds., The Western North Atlantic Region, Volume M, GSA DNAG, p. 351-378.

Le Pichon, X., and Angelier, J., 1979, The Hellenic arc and trench system: A key to the neotectonic evolution of the eastern Mediterranean area, *Tectonophysics, 60*, 1-42.

Lonergan, L., and White, N., 1997, Origin of the Betic-Rif mountain belt: *Tectonics, v. 16*, p. 504-522.

Martínez-Martínez, J. M., Booth-Rea, G., Azañón, J. M. and Torcal, F., 2006, Active transfer fault zone linking a segmented extensional system (Betics, southern

Spain): Insight into heterogeneous extension driven by edge delamination: *Tectonophysics, v. 422*, p 159-173.

McCaffrey, R. (2002), Crustal block rotations and plate coupling, in Plate Boundary Zones, Geodynamics Series 30, S. Stein and J. Freymueller, editors, 101-122, AGU.

McClusky et al., 2000, GPS constraints on plate kinematics and dynamics in the eastern Mediterranean and Caucasus, *J. Geophys. Res*., *105,* 5695-5719.

McClusky, S., Reilinger, R., Mahmoud, S., Ben Sari, D., and Tealeb, A., 2003, GPS constraints on Africa (Nubia) and Arabia plate motions: *Geophys. J. Int., v. 155*, p. 126-138.

Meghraoui, M., Outtani, F., Choukri, A., and Frizon de Lamotte, D., 1998, Coastal tectonics across the South Atlas thrust front and the Agadir active zone, Morocco: *Geol. Soc. London, Spec. Publ., v. 146*, p. 239-253.

Moratti, G., Piccardi, L., Vannucci, G., Bleardinelli, M.E., Dahmani, M., bendkik, A., and Chenakeb, M., 2003, The 1755 "Meknes" earthquake (Morocco): Field data and geodynamic implications: *J. Geodynamics, v. 36*, p. 305-322.

Morel, J.L., and Meghraoui, M., 1996, Goringe-Alboran-Tell tectonic zone; a transpression system along the Africa-Eurasia plate boundary: *Geology, v. 24*, p. 755-758.

Platt, J.P., and Vissers, R.L.M., 1989, Extensional collapse of thickened continental lithosphere; a working hypothesis for the Alboran Sea and Gibraltar Arc: *Geology, v. 17*, p. 540-543.

Platt, J.P., and Whitehouse, M.J., 1999, Early Miocene high-temperature metamorphism and rapid exhumation in the Betic Cordillera (Spain); evidence from U-Pb zircon ages: *Earth Planet. Sci. Lett., v. 171*, p. 591-605.

Platt, J.P., Whitehouse, M.J., Kelley, S.P., Carter, A., and Hollick, L., 2003, Simultaneous extensional exhumation across the Alboran Basin; implications for the causes of late orogenic extension: *Geology, v. 31*, p. 251-254.

Rebai, S., Philip, H., and Taboada, A., 1992, Modern tectonic stress field in the Mediterranean region; evidence for variation in stress directions at different scales: *Geophys. J. Int., v. 110*, p. 106-140.

Royden, L.H., 1993, Evolution of retreating subduction boundaries formed during continental collision: *Tectonics, v. 12*, p. 629-638.

Savage, J., and Burford, R., 1973, Geodetic determination of relative plate motion in Central California: J. Geophys. Res., v. 78, p. 832-845.

Seber, D., Barazangi, M., Ibenbrahim, A., and Demnati, A., 1996, Geophysical evidence for lithospheric delamination beneath the Alboran Sea and Rif-Betic mountains: *Nature, v. 379*, p. 785-790.

Stich, D., Ammon, C.J., and Morales, J., 2003, Moment tensor solutions for small and moderate earthquakes in the Ibero-Maghreb region: *J. Geophys. Res., v. 108*, p. 20.

Tahayt, A., et al., Present-day movements of tectonic blocks in the western Mediterranean from GPS measurements 1999-2005, *Comptes Rendus de l'Académie des Sciences* (in French with abridged English Version), doi:10.1016/j.crte.2008.02.003, 2008.

Watts, A.B., Platt, J., and Buhl, P., 1993, Tectonic evolution of the Alboran Sea: Basin Research, v. 5, p. 153-177.

Figure Captions

Table 1. GPS velocities in an Africa-fixed and Eurasia-fixed reference frame (as determined in this study), 1-sigma uncertainties (σ), and correlation between the east and north components of velocity (RHO). Sites used to estimate Euler vectors are identified as * = Nubia, + = Eurasia.

Figure 1. Seismotectonic and topographic/bathymetric (SRTM30 PLUS) map of the westernmost Mediterranean region. Black lines are mapped faults. Three hypotheses for the geometry of the plate boundary are show in red (Klitgord and Schouten, 1986), green (Bird, 2003), and blue (Gutscher, 2004). Crustal earthquake focal mechanisms are from Harvard catalog (magnitudes 5–6.5, 1976 – 2008). Seismicity is from National Earthquake Information Center catalog crustal earthquakes with magnitudes from 3 to 6.5 (1976 – 2008). MA = Middle Atlas; Alb—Alboran Sea.

Figure 2a. GPS site velocities with respect to Nubia and 95% confidence ellipses. Heavy dashed lines show locations of profiles shown in Figure 3 with the widths of the profiles indicated by lighter dashed lines. Focal mechanism indicates the location of the Feb. 2004 Al Hoceima earthquake. Base map as in Figure 1.

Figure 2b. GPS site velocities with respect to Eurasia and 95% confidence ellipses.

Format as in Figure 2a.

435

Figure 3. East and North component of the residuals in our Africa reference frame for sites on the African plate (grey triangles), and in our Eurasia reference frame for the sites on the Eurasian plate (black circles).

440 **Figure 4.** Profiles 1 and 2 (see Figure 2a). a and d: Component of velocities and 1-sigma uncertainties along the direction of plate motion (normal to profile). b and e: Component of velocities and 1-sigma uncertainties normal to the direction of plate motion (i.e., parallel to profiles). The interseismic deformation predicted by elastic block models is shown for the three main hypothesized plate boundaries (Red= Klitgord and Schouten,
445 1986; Green= Bird, 2003; Blue= Gutscher, 2004, see Figure 1 for geometry). The pink line is for a model with a central Rif block (see Figure 4 for geometry). c and f: Topography and interpretative cross section along profiles 1 and 2. CC= continental crust, LM= lithospheric mantle, OC= Ocean crust, LVA= low velocity, high attenuation seismic anomaly (Calvert et al., 2000).

450

Figure 5. Map showing elastic block model for the Africa-Eurasia plate boundary in the western Mediterranean for our preferred model. GPS residual velocities lower than their 95% confidence ellipses are shown by white dots, those higher than their 95% confidence uncertainties are depicted with red ellipses. Faults are vertical and assigned locking
455 depths of 15 km except for the faults south of the Rif that have a 30° dip down to the N. Numbers show fault strike slip and fault normal slip rates in mm/yr (fault normal

component in brackets; negative for left-lateral and compression). Slip rates are averages along each segment. White modeled faults indicate segments with fault-normal compression, and grey extension. Formal uncertainties on model slip rates are ~ 1 mm/yr. Base map as in Figure 1.

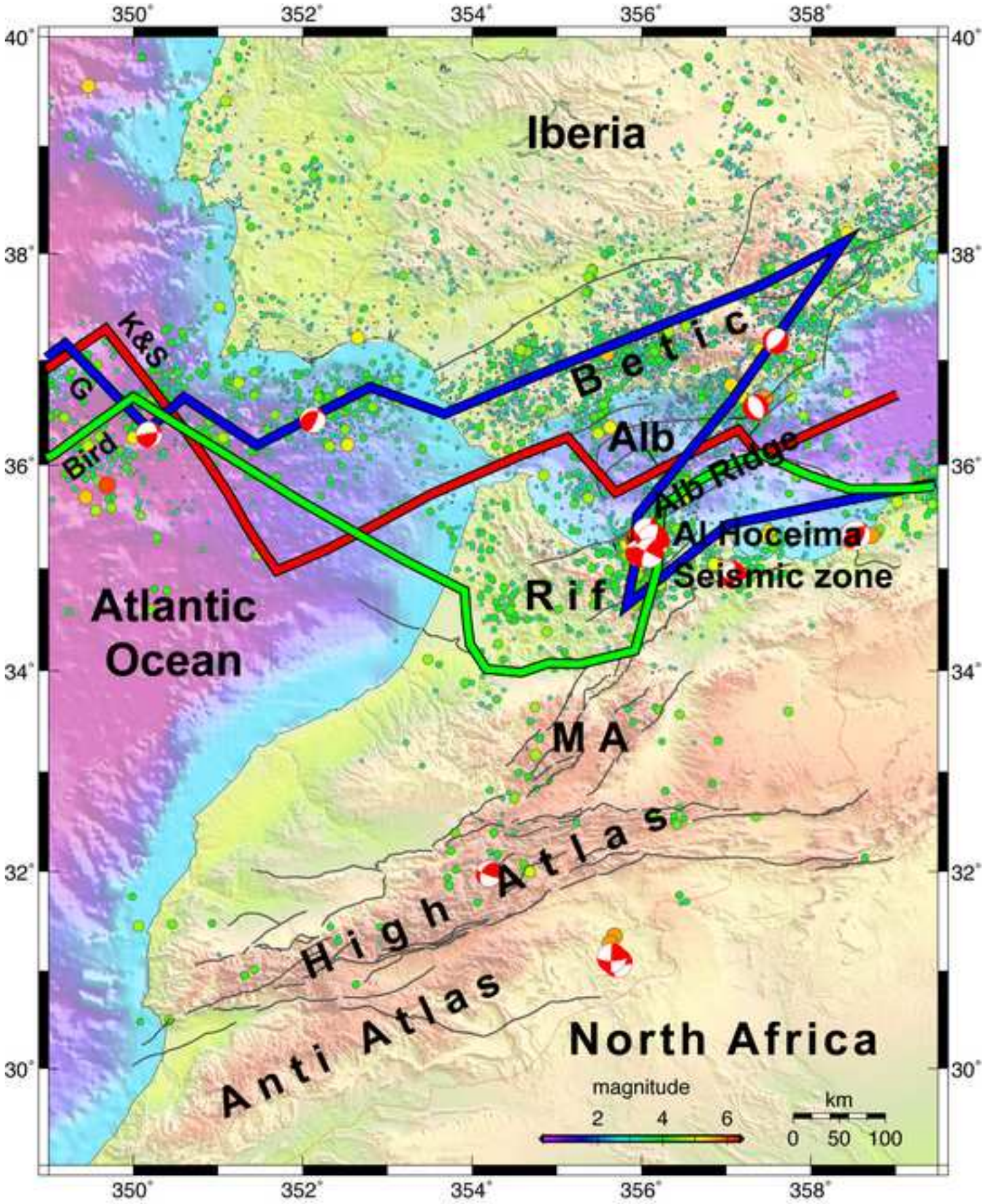

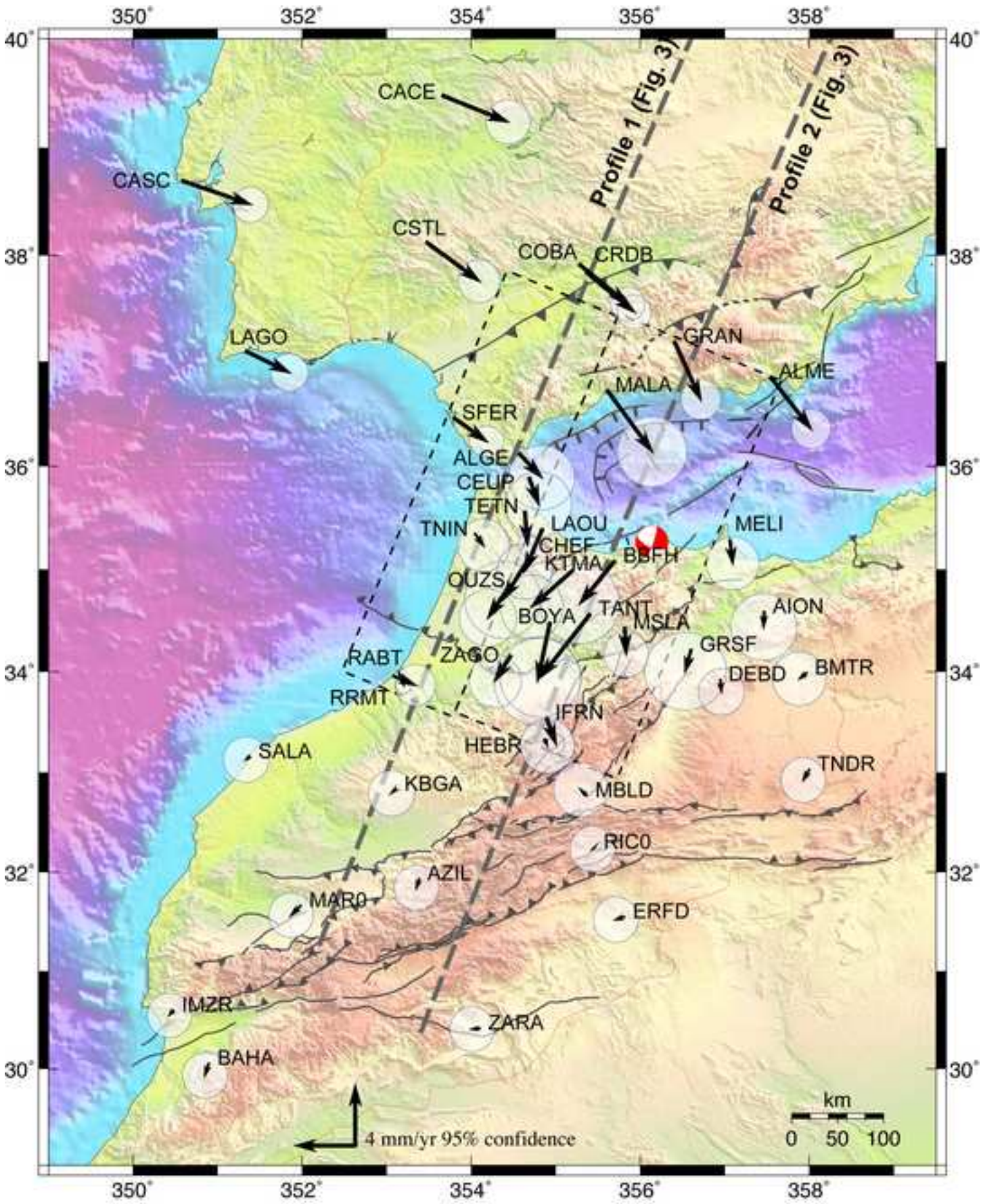

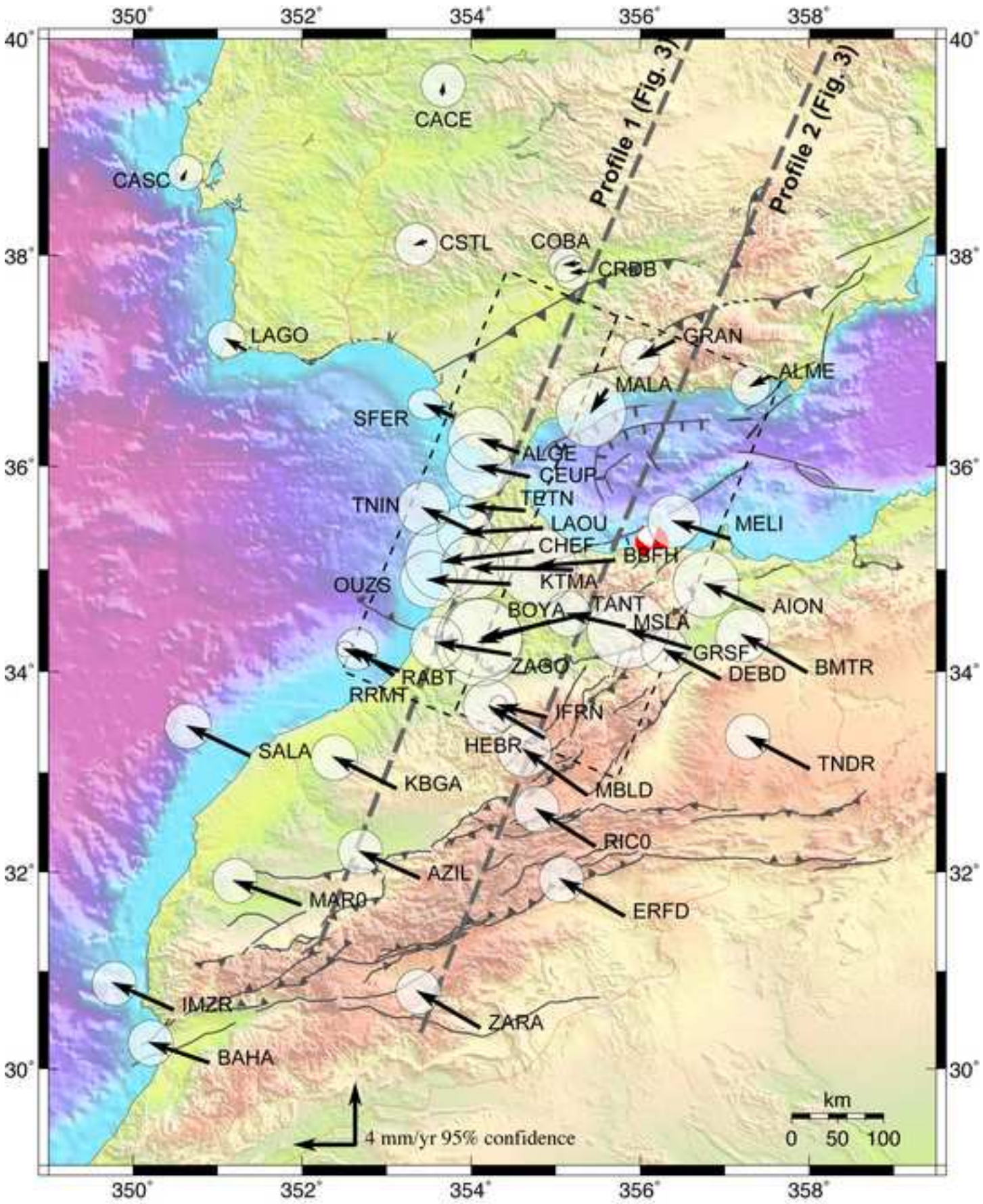

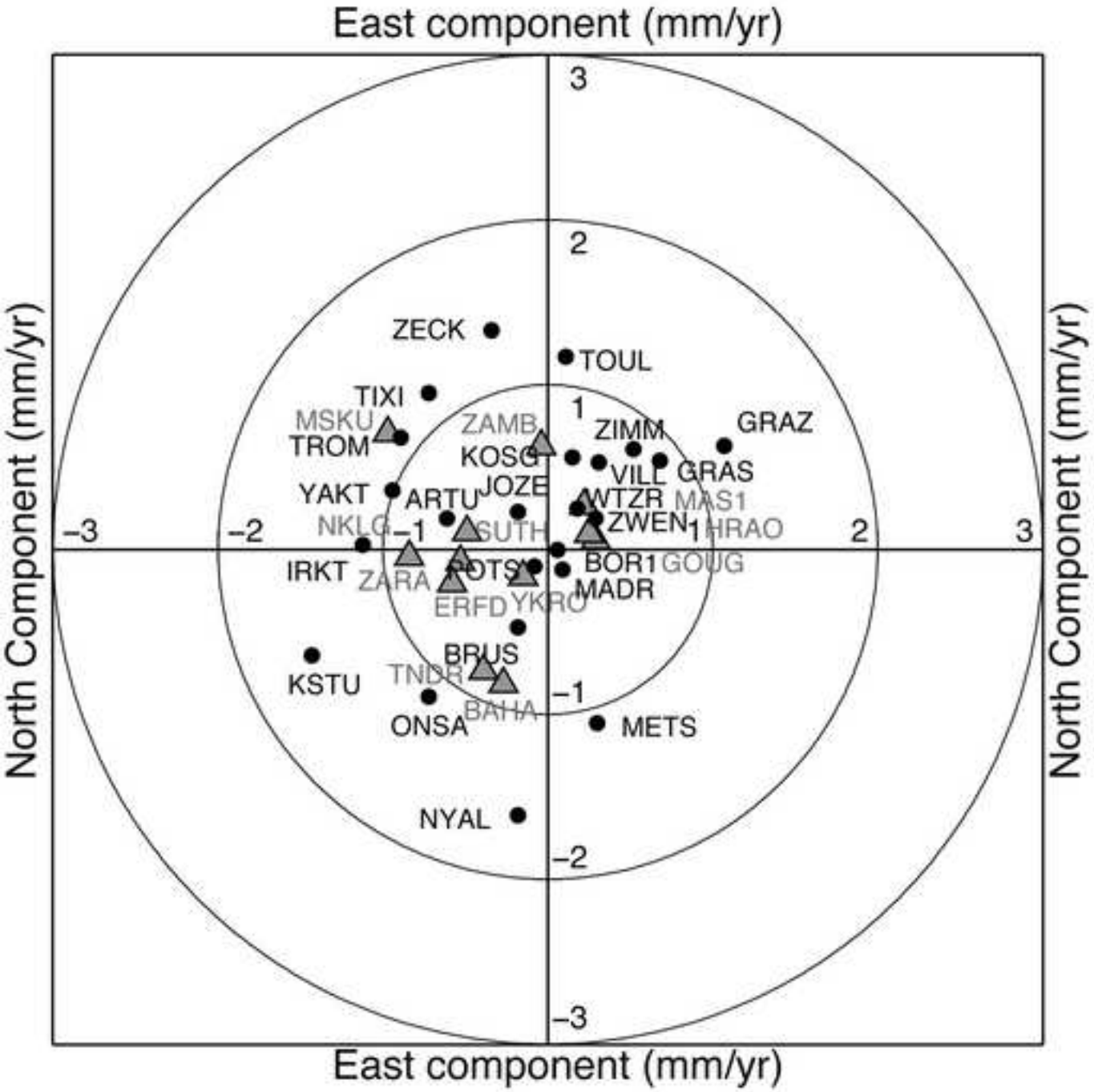

Figure 4

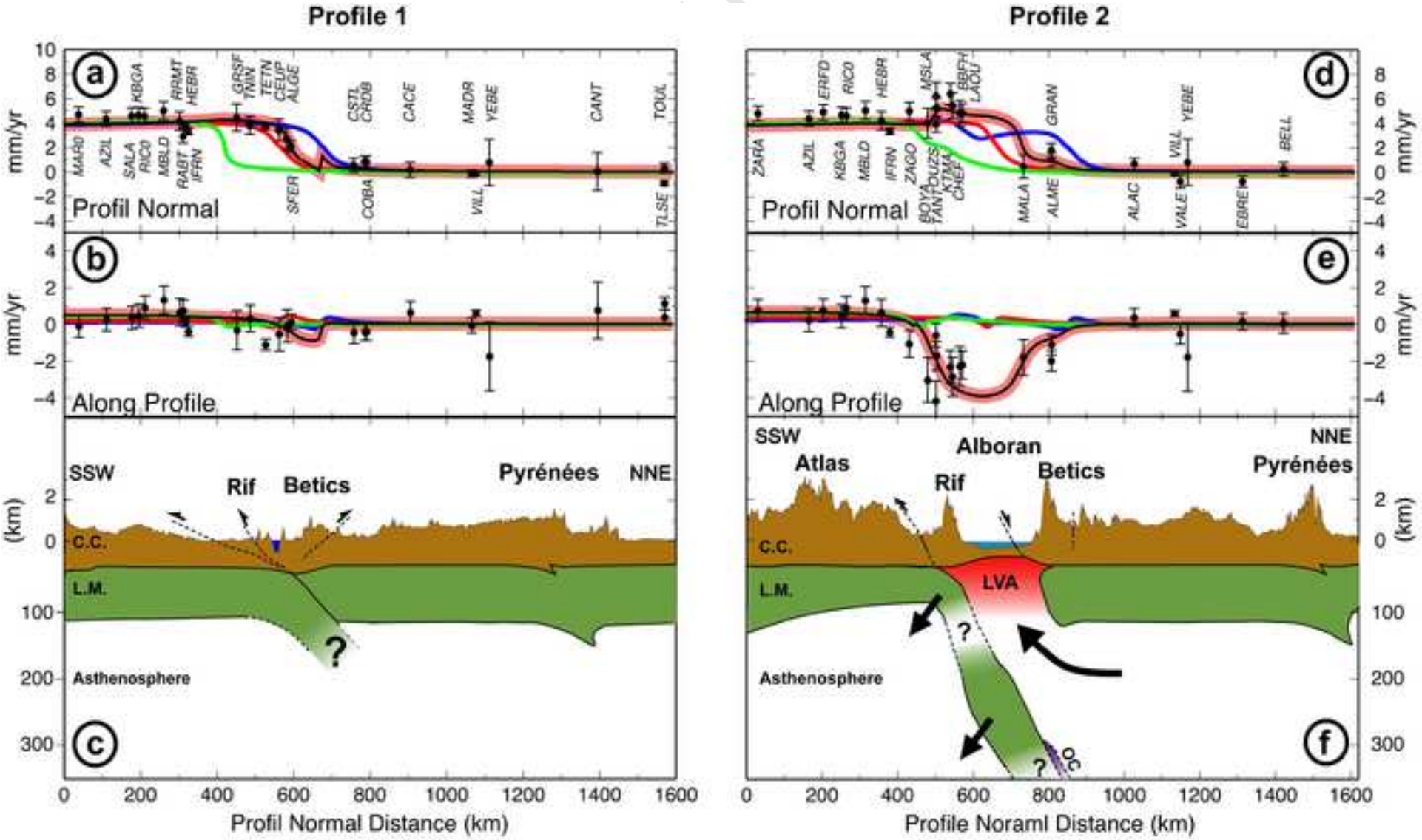
Profile 1
Profile 2
a
b
c
d
e
f
Profil Normal
Along Profile
mm/yr
SSW
NNE
Rif
Betics
Pyrénées
Atlas
Alboran
C.C.
L.M.
LVA
Asthenosphere
(km)
Profil Normal Distance (km)
Profile Noraml Distance (km)
MARO
AZIL
SALA
RICO
MBLD
RABT
IFRN
KBGA
RRMT
HEBR
GRSF
TNIN
TETN
CEUP
ALGE
SFER
CSTL
CRDB
COBA
CACE
MADR
VILL
YEBE
CANT
TLSE
TOUL
ZARA
ERFD
MSLA
BBFH
LAOU
ZAGO
BOYA
TANT
OUZS
KTMA
CHEF
GRAN
MALA
ALME
ALAC
VALE
EBRE
BELL

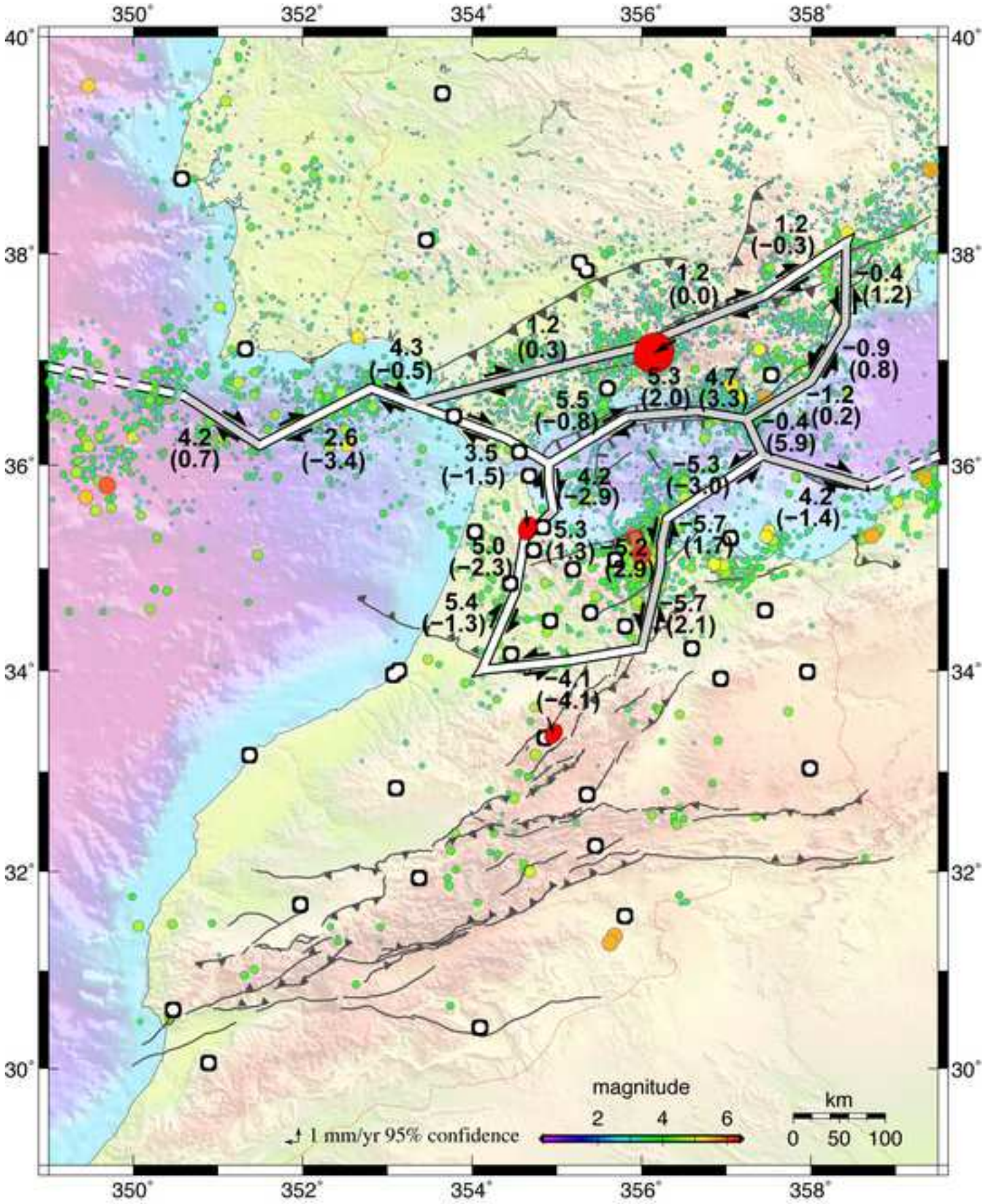

Table 1:

		Africa-fixed		Eurasia-fixed					
long. (°E)	lat. (°N)	E Vel. (mm/yr)	N Vel (mm/yr)	E Vel (mm/yr)	N Vel (mm/yr)	E σ (mm/yr)	N σ (mm/yr)	RHO	Site
359.662	39.481	4.75	-3.82	0.56	-0.76	0.54	0.54	0.044	VALE
359.519	38.339	3.66	-2.45	-0.45	0.59	0.49	0.50	0.053	ALAC
358.315	55.213	4.39	-7.52	-0.81	-4.60	1.40	1.45	0.011	MORP
357.967	33.986	-0.49	-0.39	-4.31	2.50	0.74	0.74	0.024	BMTR
357.541	36.853	2.74	-3.51	-1.32	-0.67	0.54	0.54	0.051	ALME
357.467	34.588	-0.04	-1.03	-3.92	1.80	0.91	0.92	0.028	AION
357.061	35.290	0.19	-1.60	-3.76	1.19	0.73	0.73	0.031	MELI
356.966	35.940	1.61	3.54	-2.40	6.32	1.30	1.30	0.045	ALBO
356.945	33.919	0.08	-0.81	-3.76	1.97	0.63	0.64	0.033	DEBD
356.603	34.216	-0.39	-1.46	-4.27	1.28	1.13	1.07	0.020	GRSF
356.405	37.190	1.78	-3.92	-2.34	-1.20	0.55	0.56	0.051	GRAN
356.202	43.472	4.81	-1.98	0.23	0.72	1.54	1.55	0.027	CANT
355.816	34.432	0.10	-1.80	-3.82	0.86	0.62	0.63	0.039	MSLA
355.699	35.081	-1.29	-3.05	-5.26	-0.40	1.08	1.08	0.020	BBFH
355.606	36.726	3.05	-4.15	-1.05	-1.51	0.96	0.97	0.022	MALA
355.465	32.255	-0.18	-0.14	-3.93	2.49	0.62	0.63	0.053	RIC0
355.404	34.565	-3.35	-4.27	-7.28	-1.65	1.11	1.10	0.023	TANT
355.366	32.769	-0.41	0.42	-4.20	3.03	0.74	0.75	0.034	MBLD
355.359	37.841	3.25	-2.70	-0.95	-0.09	0.47	0.47	0.073	CRDB
355.279	37.916	3.29	-2.69	-0.92	-0.09	0.47	0.47	0.073	COBA
355.198	34.987	-2.77	-2.44	-6.75	0.15	0.87	0.88	0.022	KTMA
354.931	34.485	-0.84	-3.96	-4.78	-1.39	1.20	1.21	0.024	BOYA
354.892	33.540	0.63	-1.75	-3.23	0.81	0.24	0.27	0.278	IFRN
354.869	33.333	0.19	-0.46	-3.66	2.10	0.74	0.75	0.032	HEBR
354.845	35.395	-1.23	-2.89	-5.25	-0.33	0.76	0.76	0.032	LAOU
354.734	35.173	-2.06	-3.25	-6.06	-0.71	1.05	1.06	0.036	CHEF
354.683	35.891	0.66	-1.82	-3.40	0.71	0.91	0.90	0.044	CEUP
354.637	35.562	0.17	-2.25	-3.87	0.28	0.25	0.32	0.213	TETN
354.566	36.121	1.53	-1.63	-2.56	0.89	0.91	0.89	0.042	ALGE
354.469	34.158	-1.06	-1.72	-4.99	0.80	0.72	0.73	0.035	ZAGO
354.461	34.850	-1.51	-2.23	-5.49	0.29	0.79	0.79	0.029	OUZS
354.042	35.351	0.59	-0.82	-3.45	1.65	0.72	0.73	0.035	TNIN

353.794	36.464	2.22	-1.60	-2.50	0.85	0.48	0.42	0.085	SFER
353.658	39.479	4.44	-1.78	0.08	0.65	0.61	0.61	0.041	CACE
353.468	38.123	3.58	-2.64	-0.69	-0.23	0.58	0.59	0.057	CSTL
353.384	31.934	-0.19	-0.62	-3.96	1.78	0.61	0.62	0.057	AZIL
353.146	33.998	0.33	-0.91	-3.62	1.47	0.23	0.22	0.365	RABT
353.110	32.834	-0.31	-0.28	-4.16	2.09	0.64	0.63	0.053	KBGA
353.080	33.958	1.48	-0.62	-2.47	1.74	0.56	0.57	0.051	RRMT
351.982	31.665	-0.65	-0.66	-4.43	1.59	0.61	0.62	0.053	MARO
351.601	43.364	9.13	-2.63	4.42	-0.42	0.51	0.51	0.053	ACOR
351.411	41.106	4.93	-2.11	0.38	0.07	0.58	0.58	0.044	GAIA
351.381	33.162	-0.25	-0.21	-4.16	1.98	0.63	0.63	0.044	SALA
351.332	37.099	2.96	-1.45	-1.28	0.73	0.52	0.52	0.066	LAGO
350.581	38.693	4.62	-1.60	0.24	0.50	0.49	0.49	0.075	CASC
350.119	-40.349	0.29	0.07	3.86	2.11	0.29	0.37	0.299	GOUG*
20.810	-32.380	-0.49	0.12	1.30	5.09	0.27	0.35	0.108	SUTH*
344.367	27.764	0.22	0.28	-3.32	1.69	0.19	0.25	0.578	MAS1*
13.552	-1.632	-0.97	0.72	-1.46	5.09	0.81	0.73	0.026	MSKU*
9.672	0.354	-0.84	-0.03	-1.49	4.00	0.27	0.35	0.209	NKLG*
354.760	6.871	-0.15	-0.15	-1.49	2.40	0.36	0.30	0.261	YKRO*
27.687	-25.890	0.25	0.11	1.31	5.57	0.15	0.34	0.088	HRAO*
28.311	-15.426	-0.04	0.64	0.33	6.13	0.65	0.69	0.011	ZAMB*
354.102	30.415	-0.53	-0.06	-4.15	2.42	0.61	0.62	0.058	ZARA*
350.898	30.053	-0.27	-0.80	-3.93	1.33	0.62	0.63	0.060	BAHA*
355.813	31.549	-0.58	-0.19	-4.25	2.47	0.62	0.63	0.055	ERFD*
357.997	33.031	-0.39	-0.72	-4.14	2.17	0.61	0.62	0.047	TNDR*
12.879	49.144	4.35	-4.06	0.18	0.25	0.12	0.10	0.282	WTZR+
5.810	52.178	4.85	-3.10	0.15	0.56	0.18	0.18	0.119	KOSG+
4.359	50.798	4.52	-3.99	-0.18	-0.47	0.23	0.15	0.134	BRUS+
15.493	47.067	4.99	-3.91	1.07	0.63	0.12	0.10	0.322	GRAZ+
36.759	55.699	2.96	-5.77	0.29	0.19	1.53	1.87	-0.001	ZWEN+
355.750	40.429	4.47	-2.77	0.09	-0.12	0.27	0.44	0.115	MADR+
356.048	40.444	4.68	-2.15	0.31	0.53	0.22	0.15	0.391	VILL+
21.032	52.097	3.62	-4.75	-0.18	0.23	0.13	0.09	0.092	JOZE+
6.921	43.755	4.86	-3.23	0.68	0.54	0.16	0.14	0.338	GRAS+
7.465	46.877	4.86	-3.22	0.52	0.61	0.15	0.11	0.348	ZIMM+
13.066	52.379	4.23	-4.43	-0.08	-0.10	0.43	0.42	0.011	POTS+
17.073	52.277	4.12	-4.66	0.06	0.00	0.18	0.10	0.091	BOR1+

18.938	69.663	3.55	-4.13	-0.89	0.68	0.31	0.17	-0.076	TROM+
11.926	57.395	3.87	-5.11	-0.72	-0.89	0.11	0.10	0.016	ONSA+
24.395	60.217	4.11	-6.27	0.30	-1.05	0.10	0.09	-0.095	METS+
104.316	52.219	-4.24	-4.85	-1.12	0.03	0.23	0.17	-0.459	IRKT+
92.794	55.993	-3.87	-6.30	-1.43	-0.64	0.30	0.25	-0.132	KSTU+
129.680	62.031	-6.03	-2.14	-0.94	0.36	0.63	0.51	-0.078	YAKT+
58.560	56.430	0.07	-6.40	-0.61	0.19	0.17	0.12	-0.017	ARTU+
128.866	71.634	-6.26	-1.65	-0.72	0.95	0.28	0.21	-0.286	TIXI+
41.565	43.788	1.70	-4.85	-0.34	1.33	0.13	0.12	-0.067	ZECK+
1.481	43.561	4.51	-2.08	0.11	1.17	0.41	0.32	0.073	TOUL+
11.865	78.930	4.91	-5.83	-0.18	-1.61	0.16	0.22	-0.252	NYAL+